

Two-year clinical, angiographic, and serial optical coherence tomographic follow-up after implantation of an everolimus-eluting bioresorbable scaffold and an everolimus-eluting metallic stent: insights from the randomised ABSORB Japan trial



Yoshinobu Onuma¹, MD; Yohei Sotomi², MD; Hiroki Shiomi³, MD; Yukio Ozaki⁴, MD; Atsuro Namiki⁵, MD; Satoshi Yasuda⁶, MD; Takafumi Ueno⁷, MD; Kenji Ando⁸, MD; Jungo Furuya⁹, MD; Keiichi Igarashi⁹, MD; Ken Kozuma¹⁰, MD; Kengo Tanabe¹¹, MD; Hajime Kusano¹², PhD; Richard Rapoza¹², PhD; Jeffrey J. Popma¹³, MD; Gregg W. Stone¹⁴, MD; Charles Simonton¹², MD; Patrick W. Serruys¹⁵, MD; Takeshi Kimura^{3*}, MD, PhD

1. Thoraxcenter, Erasmus MC, Rotterdam, The Netherlands; 2. Academic Medical Center, Amsterdam, The Netherlands; 3. Kyoto University Hospital, Kyoto, Japan; 4. Department of Cardiology, Fujita Health University Hospital, Toyoake, Japan; 5. Department of Cardiology, Kanto Rosai Hospital, Kawasaki, Japan; 6. Department of Cardiovascular Medicine, National Cerebral and Cardiovascular Center, Osaka, Japan; 7. Department of Medicine, Division of Cardiovascular Medicine, Kurume University School of Medicine, Kurume, Japan; 8. Division of Cardiology, Kokura Memorial Hospital, Kitakyushu, Japan; 9. Cardiovascular Center, Japan Community Health Care Organization Hokkaido Hospital, Hokkaido, Japan; 10. Teikyo University Hospital, Tokyo, Japan; 11. Mitsui Memorial Hospital, Tokyo, Japan; 12. Abbott Vascular, Santa Clara, CA, USA; 13. Beth Israel Deaconess Medical Center, Boston, MA, USA; 14. Columbia University Medical Center, New York-Presbyterian Hospital, and the Cardiovascular Research Foundation, New York, NY, USA; 15. International Centre for Circulatory Health, NHLI, Imperial College London, London, United Kingdom

GUEST EDITOR: Tommaso Gori, MD, PhD; Zentrum für Kardiologie, Universitätsmedizin Mainz, University Medical Center, Mainz and DZHK Rhein-Main, Germany.

This paper also includes supplementary data published online at: http://www.pcronline.com/eurointervention/106th_issue/180

KEYWORDS

- everolimus-eluting bioresorbable scaffold
- everolimus-eluting metallic stent
- optical coherence tomography
- randomised trial

Abstract

Aims: We sought to investigate two-year clinical and serial optical coherence tomography (OCT) outcomes after implantation of a fully bioresorbable vascular scaffold (BVS) or a cobalt-chromium everolimus-eluting stent (CoCr-EES).

Methods and results: In the ABSORB Japan trial, 400 patients were randomised in a 2:1 ratio to BVS (N=266) or CoCr-EES (N=134). A pre-specified OCT subgroup (N=125, OCT-1 group) underwent angiography and OCT post procedure and at two years. Overall, the two-year TLF rates were 7.3% and 3.8% in the BVS and CoCr-EES arms (p=0.18), respectively. Very late scaffold thrombosis (VLST) beyond one year was observed in 1.6% (four cases: all in non-OCT-1 subgroups) of the BVS arm, while there was no VLST in the CoCr-EES arm. In three cases, OCT at the time of or shortly after VLST demonstrated strut discontinuities, malapposition and/or uncovered struts. However, the vessel healing by two-year OCT was nearly complete in both BVS and CoCr-EES arms with almost fully covered struts, and minimal malapposition. The flow area by two-year OCT was smaller in the BVS arm than in the CoCr-EES arm, mainly due to tissue growth inside the device. However, there were no differences between the BVS and CoCr-EES with regard to the quality of homogenous tissues growing inside the devices.

Conclusions: The rate of TLF was numerically higher in the BVS arm than in the CoCr-EES arm, although this difference was not statistically significant. VLST was observed only in the BVS arm at a rate of 1.6% between one and two years. Further studies are mandatory to investigate the risk of BVS relative to metallic stents for VLST, and the underlying mechanisms of BVS VLST.

*Corresponding author: Department of Cardiovascular Medicine, Kyoto University Hospital, 54 Kawaharacho, Shogoin, Sako-ku, Kyoto, 606-8507, Japan. E-mail: taketaka@kuhp.kyoto-u.ac.jp

Introduction

The fully bioresorbable coronary scaffold is a new device treatment for coronary artery stenosis which provides temporary mechanical support with drug elution, potentially without the limitations of permanent metallic implants¹. The potential of this technology to induce late lumen enlargement and plaque reduction has been demonstrated in a few seminal observations up to five-year follow-up using multiple imaging modalities². The longitudinal imaging observations were, however, made in the absence of a comparator.

A recent meta-analysis of the four randomised trials (ABSORB II, III, Japan and China)²⁻⁵ comparing an everolimus-eluting polylactide bioresorbable vascular scaffold (BVS) and a cobalt-chromium everolimus-eluting metallic stent (CoCr-EES) demonstrated non-inferiority of BVS to CoCr-EES in terms of target lesion failure at one year⁶. To date, however, there is little evidence for very late events beyond one year in the context of randomised trials⁷. Actually, despite the theoretical long-term advantage of the technology, anecdotal case reports demonstrated a rare occurrence of very late stent/scaffold thrombosis (VLST) with late scaffold discontinuities on optical coherence tomography (OCT)^{8,9}. These observations warrant a report of long-term outcomes from a randomised trial to compare the rate of VLST between BVS and metallic drug-eluting stents (DES). Furthermore, a serial imaging investigation at baseline and at follow-up (with and without VLST) would provide important information to explore the mechanisms of VLST after BVS implantation.

Therefore, we conducted a randomised clinical trial comparing BVS with CoCr-EES with serial imaging substudies by OCT and intravascular ultrasound (IVUS). In the current manuscript, we report the two-year clinical outcomes in the entire study population and the serial OCT findings at post-procedure and two-year follow-up in an imaging subgroup from the ABSORB Japan trial.

Editorial, see page 1077

Methods

STUDY DESIGN AND POPULATION

ABSORB Japan was a prospective, multicentre, randomised, single-blind, active-controlled clinical trial randomising 400 patients in a 2:1 ratio to treatment with the Absorb BVS (Abbott Vascular, Santa Clara, CA, USA: N=266) or CoCr-EES (XIENCE PRIME/Xpedition; Abbott Vascular: N=134). The details of the trials have been published elsewhere⁵. All patients were maintained on a thienopyridine for at least 12 months, and aspirin indefinitely. As an imaging substudy, 125 patients were also allocated randomly to the OCT-1 group to undergo serial OCT follow-up at post-procedure and at two- and three-year follow-up.

The ethics committees approved the protocol at the participating institutions. All patients provided written informed consent and were blinded to their treatment assignment up to five-year follow-up.

ENDPOINTS AND DEFINITIONS

A complete list of endpoints is provided elsewhere⁵. Definitions of clinical endpoints, including stent/scaffold thrombosis (ST), were

based on the Academic Research Consortium criteria. Target lesion failure (TLF), the primary endpoint, was defined as a composite of cardiac death, target vessel myocardial infarction (MI), or ischaemia-driven target lesion revascularisation (ID-TLR). Independent study monitors performed on-site verification of 100% of the case report form data. Death, MI, TLR/target vessel revascularisation (TVR), and ST were adjudicated by an independent blinded clinical events committee (Harvard Clinical Research Institute, Boston, MA, USA). A data safety monitoring board monitored patient safety.

The major imaging endpoints for the present analysis included a nitrate-induced vasoreactivity test at two years on angiography and changes in average lumen (flow) area from post procedure to two years on OCT.

STENTING PROCEDURE AND TWO-YEAR IMAGING FOLLOW-UP

The details of implantation technique were previously published⁵. In the patients sub-randomised to the OCT-1 group, post-procedural OCT was performed using a frequency domain imaging system (C7/C8 system; LightLab Imaging, Westford, MA, USA or Lunawave system; Terumo Corporation, Tokyo, Japan). When significant incomplete strut apposition was observed on OCT, the performance of additional post-dilatation was allowed. Whenever additional post-dilatation was performed, angiography and OCT were repeated. At two years, coronary angiography was repeated in the same projections as at post procedure. OCT was performed in the target lesion, including 5 mm distal and 5 mm proximal to the stent/scaffold.

The imaging data were analysed in the independent core laboratories (quantitative coronary angiography [QCA]: Beth Israel Deaconess Medical Center, Boston, MA, USA, and OCT: Cardialysis, Rotterdam, The Netherlands).

OCT ANALYSIS

The final OCT recordings were analysed off-line using QIVUS software, version 3.0 (Medis, Leiden, The Netherlands). We were unable to blind the analysts to the device type because of the specific appearance of BVS and CoCr-EES struts by OCT. Taking into account the difference in optical properties of CoCr and polylactide, OCT analysis was performed using comparative methods^{10,11}. The details of OCT methods are described in **Online Appendix 1**. Definitions of OCT imaging endpoints were reported previously⁵. For the OCT endpoint analysis, stent area and derived measures are based on the abluminal stent contour⁶. Quantitative assessment of OCT was performed at 1 mm intervals, while the qualitative assessment of acute disruption and/or late discontinuities was performed frame by frame.

Statistical analysis

Two-year events were counted up to 758 days, the end of the follow-up window. The clinical endpoint was evaluated in the intent-to-treat population whereas the imaging endpoint was evaluated in the final analysis set population, excluding patients who did not receive the assigned treatment.

For binary variables, counts, percentages, and 95% confidence intervals (CI) were calculated. Pearson's chi-squared test or Fisher's exact test was performed when appropriate. Continuous variables were presented as mean and standard deviation or medians and interquartile ranges whenever appropriate. For time-to-event variables, survival curves were constructed using Kaplan-Meier estimates, and were compared by the log-rank test. All statistical analyses were performed using SAS, versions 9.2 and 9.3 (SAS Institute Inc., Cary, NC, USA).

ROLE OF THE FUNDING SOURCE

The sponsor was involved in study design, data collection, data analysis, data interpretation, and the writing of this report.

The corresponding author had full access to the analysed data in the study and accepts full responsibility for the integrity of the study and the decision to submit the manuscript for publication.

Results

CLINICAL OUTCOMES IN THE ENTIRE STUDY POPULATION

The baseline characteristics and the study flow chart of two-year follow-up are presented in **Online Table 1** and **Figure 1**. At two years, 391 patients (98%) had clinical follow-up. Almost half of the patients were on a dual antiplatelet regimen (BVS: 52.3%, CoCr-EES: 50.7%, $p=0.78$). The two-year TLF rate was not significantly different between the BVS and CoCr-EES arms. The numerically higher rate of TLF in the BVS arm was mainly driven

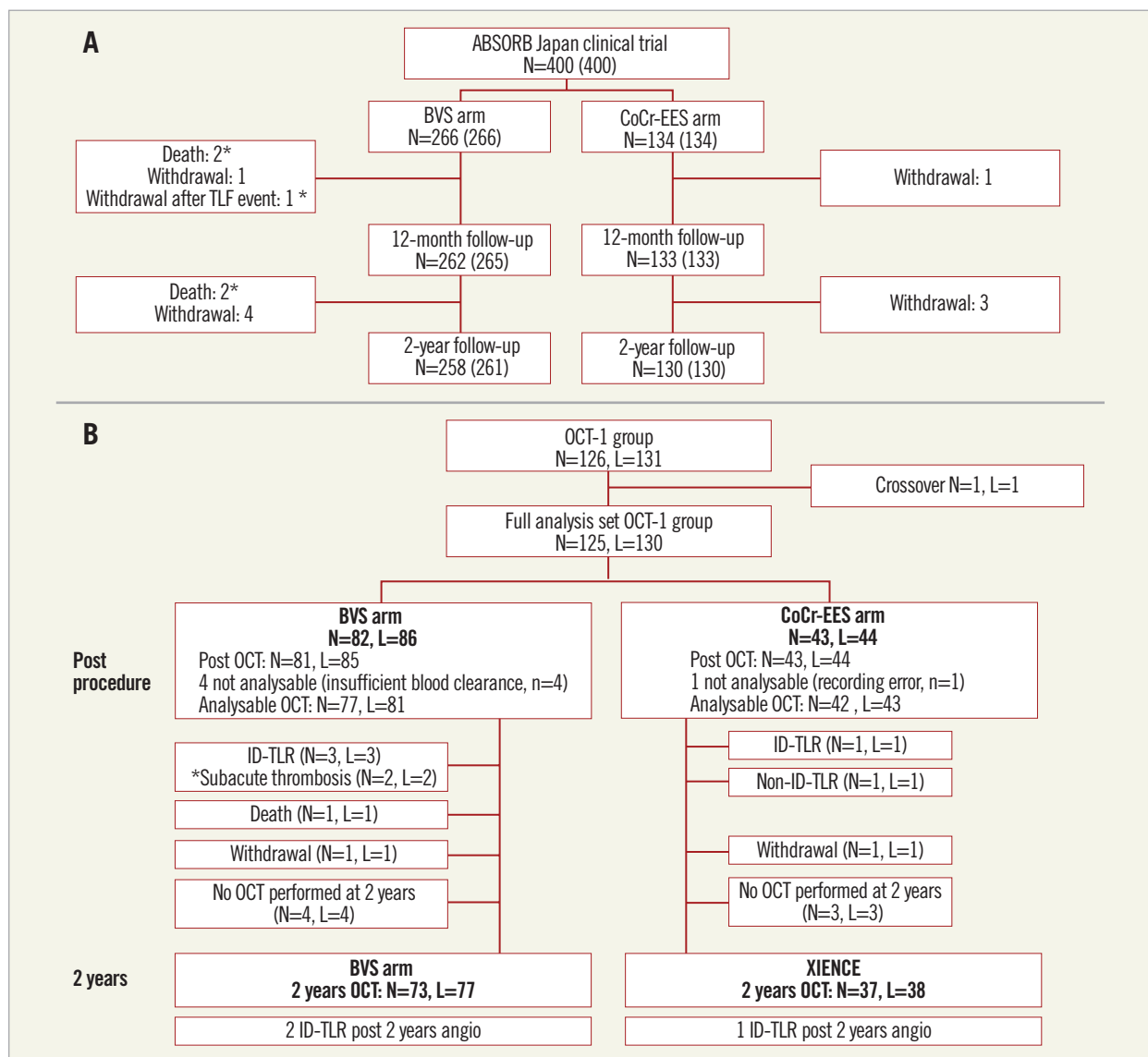


Figure 1. Study flow charts at two years. Clinical follow-up in the entire study population (A) and imaging follow-up in the OCT-1 subgroup (B). The actual number of patients analysed is indicated in brackets including subjects (*) who died or withdrew from the study after known myocardial infarction or revascularisation. BVS: bioresorbable vascular scaffold; CoCr-EES: cobalt-chromium everolimus-eluting stent; ID: ischaemia-driven; OCT: optical coherence tomography; TLR: target lesion revascularisation

by ID-TLR as well as target vessel MI. However, the rate of all TLR was similar in both arms. The definite/probable ST rates were 3.1% and 1.5% ($p=0.51$), respectively (**Table 1, Figure 2**).

From one to two years, there were four MI cases (1.6%, two non-Q-wave MI and two Q-wave MI) in the BVS arm related to VLST occurring from 494 to 679 days after the index procedure (**Table 1**).

CHARACTERISTICS OF PATIENTS WITH VLST AND OCT FINDINGS AT THE TIME OF VLST

The clinical, angiographic, and procedural characteristics, OCT findings at the time of VLST, and narratives of these four VLST cases with OCT images are presented in **Figure 3** and **Online Appendix 2**. Of note, all four VLST cases did not belong to the OCT-1 subgroup, and therefore did not undergo OCT imaging at post procedure. These four VLST cases had a relatively large angiographic reference vessel diameter, and the scaffolds were widely patent at one-year follow-up angiography in all cases. One case was not on any antiplatelet therapy at the time of VLST. On post-VLST OCT performed in three cases, malapposition and late strut discontinuities were observed in all cases (**Figure 3, Online Table 2**).

SERIAL OCT AND ANGIOGRAPHIC FINDINGS IN THE OCT-1 SUBGROUP

The baseline characteristics and the patient flow in the OCT-1 subgroup are presented in **Online Table 1** and **Figure 1**. Two patients in the OCT-1 subgroup experienced subacute ST. In one case, post-procedure OCT revealed severe underexpansion of the scaffold and a dense cluster of strut footprints, while in the other case OCT showed acceptable scaffold expansion with a small malapposition (**Figure 3, Online Appendix 3**).

Quantitative measurements of device and flow area at post procedure were comparable between the BVS and CoCr-EES arms (**Table 2**). The BVS scaffold area was more eccentric than the CoCr-EES. Malapposed struts were less frequently seen with BVS than with CoCr-EES, although the incomplete stent apposition (ISA) area was small and not different in both arms. The BVS struts were less embedded than the CoCr-EES struts. In qualitative analysis, there was no acute disruption of polymeric struts.

OCT at two years demonstrated a uniform tissue coverage in most of the lesions in both the BVS and CoCr-EES arms (**Figure 4**). The dimensions of stent and scaffold were stable over two years after implantation (**Figure 5**), while there was a trend towards greater neointimal growth with BVS than with CoCr-EES (**Table 3**).

Table 1. Clinical outcomes – composite and non-hierarchical events (intention-to-treat).

	2 years				Between 1 and 2 years [#]			
	BVS N=261	CoCr-EES N=130	Relative risk [95% CI]	p-value	BVS N=257	CoCr-EES N=130	Relative risk [95% CI]	p-value
Composite endpoints								
TLF	19 (7.3%)	5 (3.8%)	1.89 [0.72, 4.96]	0.18	8 (3.1%)	1 (0.8%)	4.05 [0.51, 32.01]	0.28
TVF	29 (11.1%)	9 (6.9%)	1.60 [0.78, 3.29]	0.19	15 (5.8%)	4 (3.1%)	1.90 [0.64, 5.60]	0.24
POCE	52 (19.9%)	16 (12.3%)	1.62 [0.96, 2.72]	0.06	30 (11.7%)	10 (7.7%)	1.52 [0.77, 3.01]	0.22
Cardiac death or MI	15 (5.7%)	4 (3.1%)	1.87 [0.63, 5.51]	0.25	6 (2.3%)	1 (0.8%)	3.04 [0.37, 24.95]	0.43
Individual endpoints								
All-cause death	4 (1.5%)	0 (0.0%)	–	0.31	2 (0.8%)	0 (0.0%)	–	0.55
Cardiac death	1 (0.4%)	0 (0.0%)	–	1	1 (0.4%)	0 (0.0%)	–	1
All MI	14 (5.4%)	4 (3.1%)	1.74 [0.59, 5.19]	0.31	5 (1.9%)	1 (0.8%)	2.53 [0.30, 21.42]	0.67
Target vessel MI	13 (5.0%)	4 (3.1%)	1.62 [0.54, 4.87]	0.38	4 (1.6%)	1 (0.8%)	2.02 [0.23, 17.92]	0.67
Target vessel QMI	6 (2.3%)	0 (0.0%)	–	0.18	3 (1.2%)	0 (0.0%)	–	0.55
Target vessel NQMI	7 (2.7%)	4 (3.1%)	0.87 [0.26, 2.92]	1	1 (0.4%)	1 (0.8%)	0.51 [0.03, 8.02]	1
All coronary revascularisation	45 (17.2%)	15 (11.5%)	1.49 [0.87, 2.58]	0.14	28 (10.9%)	10 (7.7%)	1.42 [0.71, 2.83]	0.32
All TVR	25 (9.6%)	10 (7.7%)	1.25 [0.62, 2.51]	0.54	14 (5.4%)	6 (4.6%)	1.18 [0.46, 3.00]	0.73
ID-TVTR	24 (9.2%)	7 (5.4%)	1.71 [0.76, 3.86]	0.19	13 (5.1%)	4 (3.1%)	1.64 [0.55, 4.94]	0.37
All TLR	15 (5.7%)	7 (5.4%)	1.07 [0.45, 2.55]	0.88	8 (3.1%)	4 (3.1%)	1.01 [0.31, 3.30]	1
ID-TLRR	14 (5.4%)	3 (2.3%)	2.32 [0.68, 7.94]	0.16	7 (2.7%)	1 (0.8%)	3.54 [0.44, 28.47]	0.28
Scaffold/stent thrombosis								
Definite	8 (3.1%) [*]	1 (0.8%)		0.28	4 (1.6%) ^{**}	0 (0.0%)		0.31
Definite/probable	8 (3.1%) [*]	2 (1.5%)		0.51	4 (1.6%) ^{**}	0 (0.0%)		0.31

*N=257; **N=256. # Patients with second or third event are also counted. BVS: bioresorbable vascular scaffold; CoCr-EES: cobalt-chromium everolimus-eluting stent; ID: ischaemia-driven; MI: myocardial infarction; NQMI: non-Q-wave MI; POCE: patient-oriented composite endpoint; QMI: Q-wave MI; TLF: target lesion failure; TLR: target lesion revascularisation; TVF: target vessel failure; TVR: target vessel revascularisation

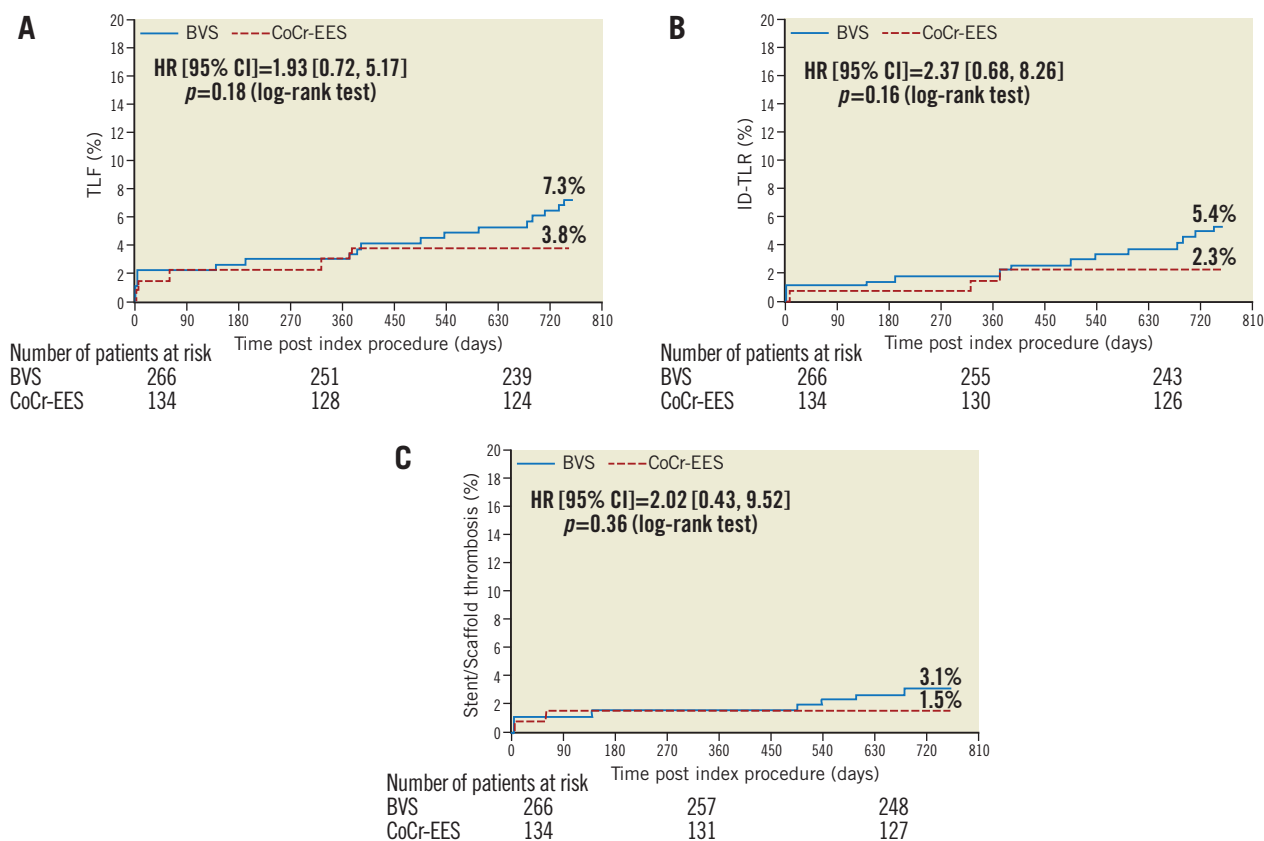


Figure 2. Kaplan-Meier estimates for TLF (A), ID-TLR (B) and definite or probable ST (C). BVS: bioresorbable vascular scaffold, CoCr-EES: cobalt-chromium everolimus-eluting stent; HR: hazard ratio; ID: ischaemia-driven; TLF: target lesion failure; TLR: target lesion revascularisation; ST: scaffold/stent thrombosis

As a result, the mean and minimum flow area was smaller in the BVS arm than in the CoCr-EES arm, which was consistent with the smaller in-device minimum lumen diameter by QCA (**Online Table 3**). Paired OCT data demonstrated a larger reduction of mean flow area in the BVS arm than in the CoCr-EES arm (BVS: -1.49 ± 1.13 mm² vs. CoCr-EES: -0.80 ± 0.74 mm², $p=0.001$).

The vessel healing on OCT was complete and similar in both the BVS and CoCr-EES arms. The tissue characteristics at the site of minimal scaffold/stent area were similar in both arms, with most of the characterised tissues being homogeneous (**Table 3**). Coverage of the struts was nearly complete in both arms, while ISA areas were minimal, resulting in minimal healing scores in both arms.

The serial OCT of the scaffold segment allowed the assessment of strut discontinuities, whether they were persistent or late acquired. Overhanging or stacked struts were found at two years in approximately one quarter of the BVS arm, although there was no acute strut disruption at post-procedure OCT. However, the majority of such struts were well covered and apposed (**Table 3**). In only three cases, such struts were uncovered and malapposed (**Figure 3**). There were no adverse events associated with these findings.

An angiographic vasomotion test before and after nitrate administration demonstrated no significant differences between the two arms in vasodilatation (0.06 ± 0.14 mm vs. 0.07 ± 0.17 mm, $p=0.89$).

Discussion

The present two-year follow-up of the ABSORB Japan trial demonstrated the following: (1) the rate of TLF was numerically higher in the BVS arm than in the CoCr-EES arm, although this difference was not statistically significant; (2) VLST after one year was observed in 1.6% of the BVS arm, while there was no VLST in the CoCr-EES arm; (3) in three cases, OCT at the time of or shortly after VLST demonstrated strut discontinuities, malapposition and/or uncovered struts; (4) in the imaging subgroup with serial OCT, the vessel healing on two-year OCT was complete in both the BVS and CoCr-EES arms with almost full strut coverage, minimal ISA, and homogenous in-device tissue growth.

The current study showed statistically non-different two-year TLF rates between the BVS and CoCr-EES arms. The TLF rate in the BVS arm was in parallel with the rates reported in the ABSORB cohort B and ABSORB II trials, although the event rates were numerically higher in the BVS than in the CoCr-EES arm⁸. The numerical differences in TLF rates between BVS and CoCr-EES might be derived from the low event rate in the CoCr-EES arm (3.8%), which is currently regarded as the best-in-class DES^{12,13}.

Four patients (1.6%) in the BVS arm had VLST between one and two years. There is a scarcity of data on VLST stemming from randomised trials, except for the ABSORB II trial that showed

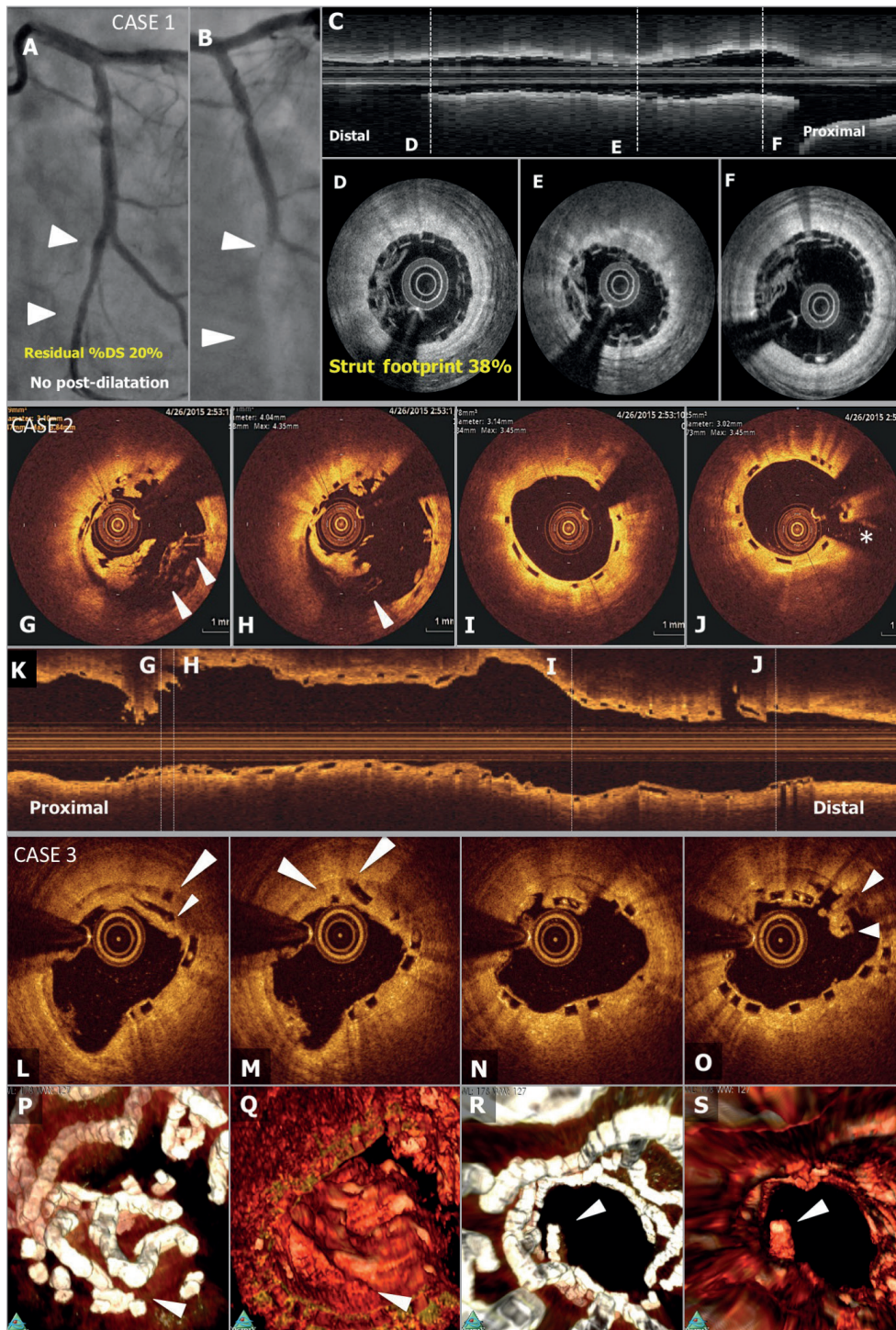


Figure 3. Representative angiographic and OCT images. *Case 1.* A case of subacute ST (A-F): a patient received a 2.5 mm BVS in a left circumflex coronary artery without post-dilatation (A). Post-procedural optical frequency domain imaging (C-F) showed severe underexpansion of the proximal part of the scaffold with a minimum lumen area of 2.48 mm² and mean scaffold area of 3.47 mm² with a high density of polymeric struts (D & E). On day 4, the patient developed subacute ST (B). The full description of the two subacute ST cases is provided in Online Appendix 3. *Case 2.* OCT images at the time of VLST on day 494 (G-K): OCT after thrombus aspiration demonstrated overhanging struts and uncovered malapposed struts (G & H). The middle and distal parts of the scaffold showed no remarkable findings (I & J). The full description of the four VLST cases is provided in Online Appendix 2. *Case 3.* A case of late strut discontinuities without any clinical sequel (L-S): OCT at two years demonstrated covered and overhanging struts (arrowheads in L & M) and malapposed and overhanging struts with back tissue bridge (arrowheads in O), indicating late discontinuities. In the corresponding 3-dimensional OCT reconstructions with (Q) or without tissue enhancement (P), two rings were overlapping with tissue coverage. One ring was protruding into the lumen from the vessel wall (R), but this was integrated in the vessel wall by tissue extending behind struts (S).

Table 2. Baseline OCT findings in the OCT-1 subgroup.

	BVS	CoCr-EES	p-value
Number of lesions evaluated	N=81	N=43	
Mean flow area (mm ²)	6.84±1.98	7.29±2.41	0.26
Minimum flow area (mm ²)	5.60±1.81	5.95±2.23	0.35
Mean abluminal scaffold/stent area (mm ²)	7.74±2.10	8.05±2.49	0.46
Minimum abluminal scaffold/stent area (mm ²)	6.55±1.99	6.90±2.44	0.40
Mean scaffold/stent eccentricity	0.86±0.04	0.88±0.03	<0.001
Minimum scaffold/stent eccentricity	0.79±0.08	0.84±0.06	<0.001
Asymmetry index of scaffold/stent	0.28±0.09	0.23±0.07	0.006
Mean lumen diameter (mm)	3.03±0.42	3.02±0.52	0.94
% Malapposed struts	2.00 (0.68, 6.37)	6.35 (3.61, 14.94)	0.005
Mean ISA area, overall (mm ²)	0.03 (0.00, 0.09)	0.06 (0.01, 0.12)	0.34
Lesion with ≥1 malapposed struts	67 [82.7]	40 [93.0]	0.17
Lesion with acute disruption	0%	–	
Median embedment depth per lesion (µm)	50 (42, 59)	84 (67, 98)	<0.001
Strut level analysis			
Number of struts analysed	N=14,633	N=9,048	
Malapposed struts	715 [4.9]	849 [9.4]	<0.001

Data area expressed as mean±SD, median (interquartile range), or number [percentage]. BVS: bioresorbable vascular scaffold; CoCr-EES: cobalt-chromium everolimus-eluting stent; ISA: incomplete strut apposition; OCT: optical coherence tomography

two-year definite VLST rates of 0.6% in the BVS arm and 0% in the CoCr-EES arm. Among the BVS registries reporting outcomes beyond one year, the reported VLST rates ranged from 0.6 to 0.8%^{8,14}, which might be slightly higher than those for CoCr-EES (approximately 0.2%)^{15,16}. The results from future pooled analyses of randomised trials would provide further insights into the risk of BVS relative to metallic DES for VLST.

In the four VLST cases, the scaffolds were widely patent at one-year angiographic follow-up, suggesting that the occurrence of VLST could relate to structural abnormalities undetectable on angiography. Due to the bioresorption, radial mechanical support of BVS decreases at ≈6 months and is minimal at 12 months. After one year, the mechanical support of BVS is almost absent. Increasing plaque proliferation, which could be induced by uncontrolled cardiovascular risks, and the progressive reduction in vessel support could facilitate such structural abnormalities. In three VLST cases, OCT at the time of or shortly after VLST demonstrated strut discontinuities, malapposition and/or uncovered struts. These findings are in line with the previous reports by Karanasos et al and Räber et al, demonstrating that incomplete lesion coverage, malapposition, strut discontinuities and underexpansion of the scaffold were frequently observed by OCT in patients presenting with definite BVS VLST. The causal relationship of such OCT abnormalities and VLST, however, still remains undetermined. Firstly, after the mechanical integrity of the scaffold disappears at

Table 3. Two-year follow-up OCT findings in the OCT-1 subgroup.

	BVS	CoCr-EES	p-value
Number of lesions evaluated	N=77	N=38	
Mean flow area (mm ²)	5.55±1.98	6.60±2.41	0.01
Minimum flow area (mm ²)	4.10±1.79	5.05±1.97	0.01
Mean abluminal scaffold/stent area (mm ²)	7.91±2.24	8.40±2.61	0.31
Minimum abluminal scaffold/stent area (mm ²)	6.31±2.05	7.11±2.42	0.07
Neointimal area (mm ²) (on top of/in-between struts)	2.08±0.66	1.82±0.67	0.051
Neointimal area (mm ²) (on top of struts)	1.10±0.52	1.03±0.59	0.52
Qualitative analysis of neointima			0.3
Homogeneous	73 [95]	34 [90]	
Heterogeneous	1 [1.3]	0 [0]	
Layered	3 [3.9]	4 [10.5]	
Mean scaffold/stent eccentricity (abluminal)	0.87±0.05	0.92±0.03	<0.001
Minimum scaffold/stent eccentricity (abluminal)	0.75±0.09	0.84±0.05	<0.001
Asymmetry index of scaffold/stent (abluminal)	0.34±0.09	0.24±0.08	<0.001
Late strut discontinuities	19 [25]	–	
Covered and apposed	13 [68]		
Covered and malapposed	1 [5]		
Uncovered and apposed	2 [11]		
Uncovered and malapposed	3 [16]		
Healing score	0.00 (0.00, 1.35)	0.00 (0.00, 1.04)	0.66
% Struts with ISA	0.10±0.45	0.24±0.65	0.19
Mean ISA area, overall (mm ²)	0.00 (0.00, 0.00)	0.00 (0.00, 0.00)	0.24
Lesion with ISA	6 [7.8]	6 [15.8]	0.19
Lesion with persistent ISA	3 [3.9]*	4 [10.5]	0.17
Lesion with late acquired ISA	2 [2.6]*	2 [5.3]	0.47
Covered struts (%)	100.0 (99.4, 100)	100 (99.7, 100)	0.44
Lesion with ≥1 uncovered struts	26 [33.8]	10 [26.3]	0.42
Lesion with ≥1 covered and malapposed struts	6 [7.8]	6 [15.8]	0.19
Lesion with ≥1 uncovered and malapposed struts	1 [1.3]	0 [0]	0.48
Strut level analysis			
Number of struts analysed	N=13,469	N=8,264	
Malapposed struts	17 [0.12]	16 [0.19]	0.22
Uncovered struts	77 [0.6]	33 [0.4]	0.08
Covered and malapposed struts	16 [0.1]	16 [0.2]	0.16
Uncovered and malapposed struts	1 [0.007]	0 [0.0]	0.43

*N=76. Data are expressed as mean±SD, median (interquartile range), or number [percentage]. BVS: bioresorbable vascular scaffold; CoCr-EES: cobalt-chromium everolimus-eluting stent; ISA: incomplete strut apposition; OCT: optical coherence tomography

six months after implantation, the scaffold structure becomes mal-leable so that wiring, thrombus aspiration, ballooning, or imaging procedure at late follow-up could induce strut discontinuities or

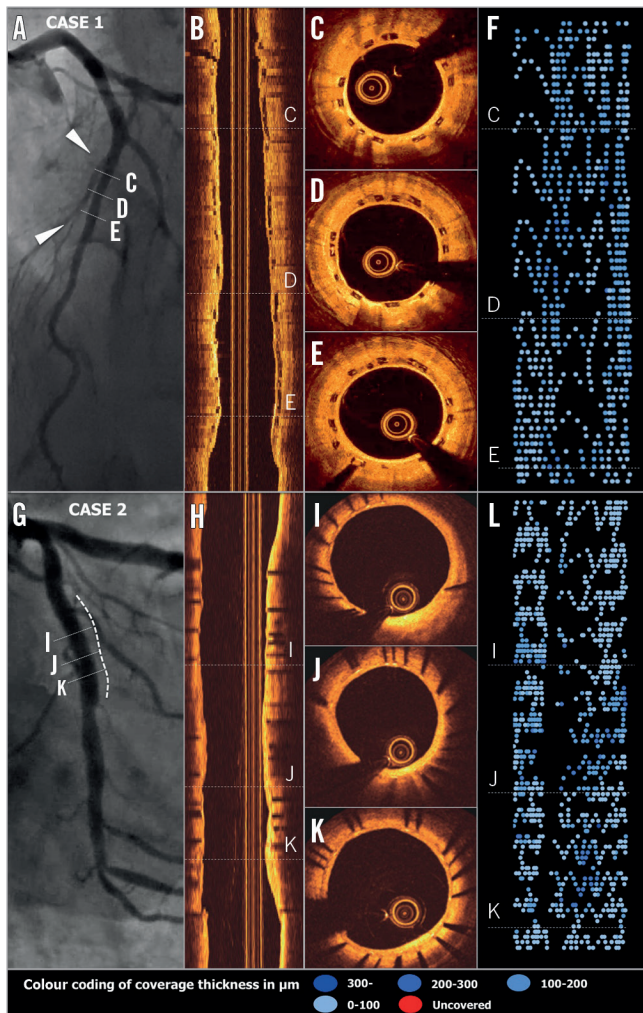


Figure 4. Typical two-year OCT images of BVS (A-F) and CoCr-EES (G-L). Case 1. A patient received a BVS in the mid left anterior descending coronary artery. On two-year OCT imaging (longitudinal view: B and cross-sections: C-E), the polymeric struts were completely covered and apposed, resulting in a healing score (HS) of 0. The foldout representation of OCT (F) illustrates graphically the distribution of neointimal thickness per strut throughout the scaffold. The extent of the thickness in microns is categorised and colour-coded at the bottom of the Figure. Case 2. A patient received a CoCr-EES in the left circumflex coronary artery. OCT at two years showed minimal neointimal hyperplasia (angiography: G, longitudinal and cross-sectional OCT: H & I-K, foldout view: L) with excellent neointimal coverage (HS=0).

malapposition¹⁷. Secondly, single OCT imaging only at the time of the event could not differentiate the persistent acute disruption/malapposition and late acquired discontinuities. In general, late discontinuities occur frequently as part of the programmed process of bioresorption¹⁷. The question remains whether the late discontinuities are bystander findings or the cause of the late event and, if so, what the trigger is to induce VLST.

At baseline, malapposed struts were less frequently observed in the BVS arm than in the CoCr-EES arm (strut-level, BVS:

4.9% vs. CoCr-EES: 9.4%), while at two years there was a low frequency of malapposition in both arms (0.12% vs. 0.19%). On OCT, malapposition is judged taking into account the thickness of the struts. As long as the same endoluminal expansion is achieved, thicker struts would have better apposition. The observed difference in malapposition rate post procedure may therefore be due to the thicker struts of BVS than those of XIENCE. Recently, Mangiameli et al reported a case of OCT-defined neoatherosclerosis observed in the BVS scaffold¹⁸. However, the vessel healing in the OCT-1 subgroup was almost complete in both the BVS and CoCr-EES arms with almost complete strut coverage, minimal ISA, and homogenous in-device tissue growth, suggesting that it would be unlikely for VLST to be causally related to ubiquitously seen adverse vascular responses to BVS. Of note, VLST did not occur in the OCT-1 subgroup where post-implantation OCT was performed. The role of post-procedure OCT in preventing VLST should be evaluated in future investigations. Approximately one half of patients still received DAPT at two years. The protocol mandated 12 months of dual antiplatelet therapy (DAPT), while DAPT after 12 months was at the discretion of investigators. The observed high rate of DAPT at two years is in line with other Japanese all-comer stent trials and may reflect Japanese clinical practice. For example, in the RESET trial (Randomized Evaluation of Sirolimus-Eluting Versus Everolimus-Eluting Stent Trial), 73% of patients were still on DAPT at two years.

The larger reduction of mean flow area and similar vasoreactivity of BVS compared to CoCr-EES were demonstrated in the present study as major imaging endpoints. The larger reduction of mean flow area could be explained by the greater neointimal growth in-between the struts related to the higher strut thickness of BVS (157 μm) than CoCr-EES (89 μm) ($p=0.051$). The neointimal area on top of the struts was comparable between both devices; the next-generation BVS with thinner strut thickness may overcome the issue of flow area reduction. Regarding the vasomotion, BVS demonstrated a larger vasoreactivity of 0.06 ± 0.14 mm than that observed in the ABSORB first-in-man trial at two years (0.034 ± 0.09 mm)¹⁹. Based on the literature²⁰, the metallic stent is not supposed to exhibit a change in dimensions after intracoronary injection of nitrate. However, CoCr-EES also showed some vasomotion, which resulted in the comparable levels of vasoreactivity between BVS and CoCr-EES. The methodological approach computing the change in lumen diameter prior to and following the intracoronary administration of nitrate with different X-ray gantry positions could have introduced confounding factors in the calibration process and blurred the difference in vasomotoricity between BVS and CoCr-EES.

Limitations

Several limitations have to be acknowledged. First, the study is severely underpowered to detect differences in clinical outcomes between BVS and CoCr-EES at two years, especially in low-frequency events. Second, the included patients mainly had

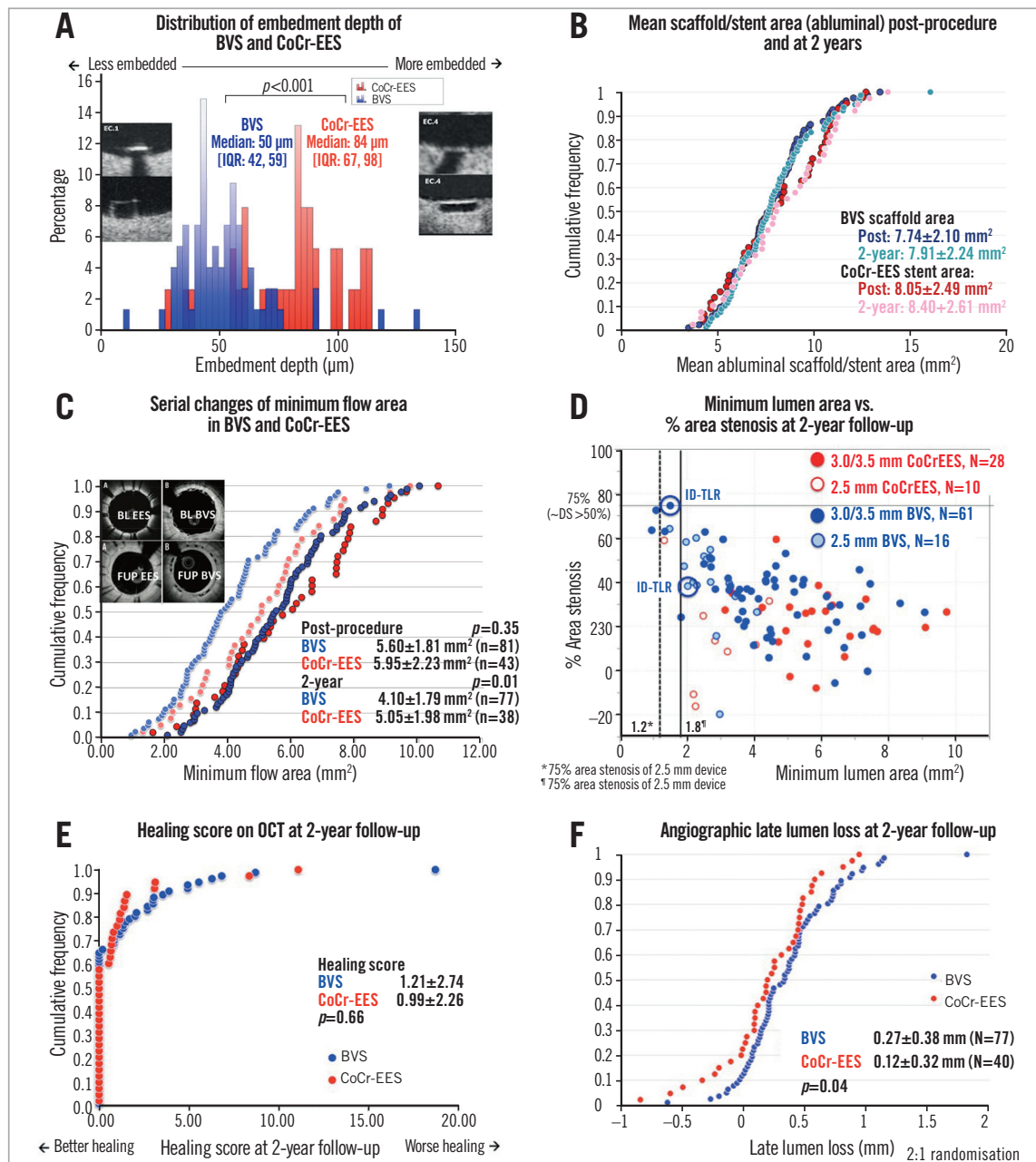


Figure 5. Quantitative OCT and angiographic analysis. A) Distribution of embedment depth of BVS and CoCr-EES on post-procedural OCT. B) Cumulative distribution function curves (CDFC) of scaffold area and stent area as assessed on OCT post procedure and at two years. C) CDFC of minimal flow area at post procedure and two years comparing BVS with CoCr-EES. D) Scatter plot of minimum lumen area and % area stenosis as assessed by OCT at two years. E) OCT healing scores at two years comparing BVS with CoCr-EES. F) CDFC of angiographic in-device late lumen loss at two years comparing BVS with CoCr-EES. BVS: bioresorbable vascular scaffold; CoCr-EES: cobalt-chromium everolimus-eluting stent

stable CAD and non-complex lesions, precluding the generalisability of the study findings to patients with complex lesions. A recent meta-analysis suggested that an ethnicity difference might confound the results of strut coverage²¹. Therefore, careful interpretation is needed when extrapolating the current results to a Western population²². The strut coverage of the current trial is, however, consistent with the ABSORB cohort B trial analysed in the same core lab. Third, the absence of VLST in the OCT-1

subgroup did not allow us to identify any OCT imaging correlates at post procedure associated with subsequent VLST.

Conclusions

In conclusion, at two years after implantation, the rate of TLF was numerically higher in the BVS arm than in the CoCr-EES arm, although this difference was not statistically significant. VLST was observed at a rate of 1.6% between one and two years

only in the BVS arm. Further studies are mandatory to investigate the risk of BVS relative to metallic stents for VLST, and the underlying mechanisms of BVS VLST.

Impact on daily practice

Scarce data are available on midterm (>1 year) outcomes after implantation of a fully bioresorbable everolimus-eluting vascular scaffold (BVS) in comparison with a cobalt-chromium everolimus-eluting stent (CoCr-EES). In the ABSORB Japan randomised trial comparing BVS and CoCr-EES, vessel healing as assessed by optical coherence tomography at two years was almost complete in both arms, with complete strut coverage and minimal strut malapposition. The two-year target lesion failure rate was not statistically different but numerically higher in the BVS arm than in the CoCr-EES arm. VLST after one year was observed in 1.6% of the BVS arm, which warrants further investigation.

Guest Editor

This paper was guest edited by Tommaso Gori, MD, PhD; Zentrum für Kardiologie, Universitätsmedizin Mainz, University Medical Center, Mainz and DZHK Rhein-Main, Germany.

Conflict of interest statement

Y. Onuma and P.W. Serruys are members of the Advisory Board of Abbott Vascular. G.W. Stone is Chairman of the Advisory Board of Abbott Vascular and a consultant to Reva Corp. J.J. Popma reports grants from Abbott Vascular and personal fees from Abbott Vascular. A. Namiki, T. Ueno, K. Ando, K. Igarashi, K. Kozuma, K. Tanabe, and T. Kimura report personal fees for advisory agreements with Abbott Vascular Japan. H. Kusano, R. Raposa and C. Simonton are employees of Abbott Vascular. The other authors have no conflicts of interest to declare. The Guest Editor, Tommaso Gori, has received speaker's honoraria from multiple companies including Abbott Vascular.

References

1. Serruys PW, Garcia-Garcia HM, Onuma Y. From metallic cages to transient bioresorbable scaffolds: change in paradigm of coronary revascularization in the upcoming decade? *Eur Heart J*. 2012;33:16-25b.
2. Serruys PW, Chevalier B, Dudek D, Cequier A, Carrie D, Iniguez A, Dominici M, van der Schaaf RJ, Haude M, Wasungu L, Veldhof S, Peng L, Staehr P, Grundeken MJ, Ishibashi Y, Garcia-Garcia HM, Onuma Y. A bioresorbable everolimus-eluting scaffold versus a metallic everolimus-eluting stent for ischaemic heart disease caused by de-novo native coronary artery lesions (ABSORB II): an interim 1-year analysis of clinical and procedural secondary outcomes from a randomised controlled trial. *Lancet*. 2015;385:43-54.
3. Ellis SG, Kereiakes DJ, Metzger DC, Caputo RP, Rizik DG, Teirstein PS, Litt MR, Kini A, Kabour A, Marx SO, Popma JJ,

McGreevy R, Zhang Z, Simonton C, Stone GW; ABSORB III Investigators. Everolimus-Eluting Bioresorbable Scaffolds for Coronary Artery Disease. *N Engl J Med*. 2015;373:1905-15.

4. Gao R, Yang Y, Han Y, Huo Y, Chen J, Yu B, Su X, Li L, Kuo HC, Ying SW, Cheong WF, Zhang Y, Su X, Xu B, Popma JJ, Stone GW; ABSORB China Investigators. Bioresorbable Vascular Scaffolds Versus Metallic Stents in Patients With Coronary Artery Disease: ABSORB China Trial. *J Am Coll Cardiol*. 2015;66:2298-309.

5. Kimura T, Kozuma K, Tanabe K, Nakamura S, Yamane M, Muramatsu T, Saito S, Yajima J, Hagiwara N, Mitsudo K, Popma JJ, Serruys PW, Onuma Y, Ying S, Cao S, Staehr P, Cheong WF, Kusano H, Stone GW; ABSORB Japan Investigators. A randomized trial evaluating everolimus-eluting Absorb bioresorbable scaffolds vs. everolimus-eluting metallic stents in patients with coronary artery disease: ABSORB Japan. *Eur Heart J*. 2015;36:3332-42.

6. Stone GW, Gao R, Kimura T, Kereiakes DJ, Ellis SG, Onuma Y, Cheong WF, Jones-McMeans J, Su X, Zhang Z, Serruys PW. 1-year outcomes with the Absorb bioresorbable scaffold in patients with coronary artery disease: a patient-level, pooled meta-analysis. *Lancet*. 2016;387:1277-89.

7. Chevalier B, Onuma Y, van Boven AJ, Piek JJ, Sabate M, Helqvist S, Baumbach A, Smits PC, Kumar R, Wasungu L, Serruys PW. Randomised comparison of a bioresorbable everolimus-eluting scaffold with a metallic everolimus-eluting stent for ischaemic heart disease caused by de novo native coronary artery lesions: the 2-year clinical outcomes of the ABSORB II trial. *EuroIntervention*. 2016 Aug 27. [Epub ahead of print]

8. Karanasos A, Van Mieghem N, van Ditzhuijzen N, Felix C, Daemen J, Autar A, Onuma Y, Kurata M, Diletti R, Valgimigli M, Kauer F, van Beusekom H, de Jaegere P, Zijlstra F, van Geuns RJ, Regar E. Angiographic and optical coherence tomography insights into bioresorbable scaffold thrombosis: single-center experience. *Circ Cardiovasc Interv*. 2015;8(5).

9. Raber L, Brugaletta S, Yamaji K, O'Sullivan CJ, Otsuki S, Koppa T, Taniwaki M, Onuma Y, Freixa X, Eberli FR, Serruys PW, Joner M, Sabate M, Windecker S. Very Late Scaffold Thrombosis: Intracoronary Imaging and Histopathological and Spectroscopic Findings. *J Am Coll Cardiol*. 2015;66:1901-14.

10. Räber L, Onuma Y, Brugaletta S, Garcia-Garcia HM, Backx B, Iniguez A, Okkels Jensen L, Cequier-Fillat À, Pilgrim T, Christiansen EH, Hofma SH, Suttorp M, Serruys PW, Sabaté M, Windecker S. Arterial healing following primary PCI using the Absorb everolimus-eluting bioresorbable vascular scaffold (Absorb BVS) versus the durable polymer everolimus-eluting metallic stent (XIENCE) in patients with acute ST-elevation myocardial infarction: rationale and design of the randomised TROFI II study. *EuroIntervention*. 2016;12:482-9.

11. Nakatani S, Sotomi Y, Ishibashi Y, Grundeken MJ, Tateishi H, Tenekecioglu E, Zeng Y, Suwannasom P, Regar E, Radu MD, Raber L, Bezerra H, Costa MA, Fitzgerald P, Prati F, Costa RA, Dijkstra J, Kimura T, Kozuma K, Tanabe K, Akasaka T, Di Mario C, Serruys PW, Onuma Y. Comparative analysis method

- of permanent metallic stents (XIENCE) and bioresorbable poly-L-lactic (PLLA) scaffolds (Absorb) on optical coherence tomography at baseline and follow-up. *EuroIntervention*. 2015 Oct 9. [Epub ahead of print].
12. Windecker S, Haude M, Neumann FJ, Stangl K, Witzenbichler B, Slagboom T, Sabate M, Goicolea J, Barragan P, Cook S, Piot C, Richardt G, Merkely B, Schneider H, Bilger J, Erne P, Waksman R, Zaugg S, Juni P, Lefevre T. Comparison of a novel biodegradable polymer sirolimus-eluting stent with a durable polymer everolimus-eluting stent: results of the randomized BIOFLOW-II trial. *Circ Cardiovasc Interv*. 2015;8:e001441.
13. Serruys PW, Silber S, Garg S, van Geuns RJ, Richardt G, Buszman PE, Kelbaek H, van Boven AJ, Hofma SH, Linke A, Klauss V, Wijns W, Macaya C, Garot P, DiMario C, Manoharan G, Kornowski R, Ischinger T, Bartorelli A, Ronden J, Bressers M, Gobbens P, Negoita M, van Leeuwen F, Windecker S. Comparison of zotarolimus-eluting and everolimus-eluting coronary stents. *N Engl J Med*. 2010;363:136-46.
14. Puricel S, Cuculi F, Weissner M, Schmermund A, Jamshidi P, Nyffenegger T, Binder H, Eggebrecht H, Munzel T, Cook S, Gori T. Bioresorbable Coronary Scaffold Thrombosis: Multicenter Comprehensive Analysis of Clinical Presentation, Mechanisms, and Predictors. *J Am Coll Cardiol*. 2016;67:921-31.
15. de la Torre Hernandez JM, Alfonso F, Gimeno F, Diarte JA, Lopez-Palop R, Perez de Prado A, Rivero F, Sanchis J, Larman M, Diaz JF, Elizaga J, Moreiras JM, Gomez Jaume A, Hernandez JM, Mauri J, Recalde AS, Bullones JA, Rumoroso JR, Del Blanco BG, Baz JA, Bosa F, Botas J, Hernandez F; ESTROFA-2 Study Group. Thrombosis of second-generation drug-eluting stents in real practice results from the multicenter Spanish registry ESTROFA-2 (Estudio Espanol Sobre Trombosis de Stents Farmacoactivos de Segunda Generacion-2). *JACC Cardiovasc Interv*. 2010;3:911-9.
16. Räber L, Magro M, Stefanini GG, Kalesan B, van Domburg RT, Onuma Y, Wenaweser P, Daemen J, Meier B, Juni P, Serruys PW, Windecker S. Very late coronary stent thrombosis of a newer-generation everolimus-eluting stent compared with early-generation drug-eluting stents: a prospective cohort study. *Circulation*. 2012;125:1110-21.
17. Onuma Y, Serruys PW, Muramatsu T, Nakatani S, van Geuns RJ, de Bruyne B, Dudek D, Christiansen E, Smits PC, Chevalier B, McClean D, Koolen J, Windecker S, Whitbourn R, Meredith I, Garcia-Garcia HM, Veldhof S, Rapoza R, Ormiston JA. Incidence and imaging outcomes of acute scaffold disruption and late structural discontinuity after implantation of the absorb Everolimus-Eluting fully bioresorbable vascular scaffold: optical coherence tomography assessment in the ABSORB cohort B Trial (A Clinical Evaluation of the Bioabsorbable Everolimus Eluting Coronary Stent System in the Treatment of Patients With De Novo Native Coronary Artery Lesions). *JACC Cardiovasc Interv*. 2014;7:1400-11.
18. Mangiameli A, Ohno Y, Attizzani GF, Capodanno D, Tamburino C. Neointerthrombosis as the cause of late failure of a bioresorbable vascular scaffold. *JACC Cardiovasc Interv*. 2015;8:633-4.
19. Serruys PW, Onuma Y, Garcia-Garcia HM, Muramatsu T, van Geuns RJ, de Bruyne B, Dudek D, Thuesen L, Smits PC, Chevalier B, McClean D, Koolen J, Windecker S, Whitbourn R, Meredith I, Dorange C, Veldhof S, Hebert KM, Rapoza R, Ormiston JA. Dynamics of vessel wall changes following the implantation of the absorb everolimus-eluting bioresorbable vascular scaffold: a multi-imaging modality study at 6, 12, 24 and 36 months. *EuroIntervention*. 2014;9:1271-84.
20. Maier W, Windecker S, Kung A, Lutolf R, Eberli FR, Meier B, Hess OM. Exercise-induced coronary artery vasodilation is not impaired by stent placement. *Circulation*. 2002;105:2373-7.
21. Iannaccone M, D'Ascenzo F, Templin C, Omede P, Montefusco A, Guagliumi G, Serruys PW, Di Mario C, Kochman J, Quadri G, Biondi-Zoccai G, Luscher TF, Moretti C, D'Amico M, Gaita F, Stone GW. Optical coherence tomography evaluation of intermediate-term healing of different stent types: systemic review and meta-analysis. *Eur Heart J Cardiovasc Imaging*. 2016 Apr 20. [Epub ahead of print].
22. Onuma Y, Kimura T, Räber L, Magro M, Girasis C, van Domburg R, Windecker S, Mitsudo K, Serruys PW; Bern-Rotterdam and j-Cypher registries. Differences in coronary risk factors, procedural characteristics, mortality and stent thrombosis between two all-comers percutaneous coronary intervention registries from Europe and Japan: a patient-level data analysis of the Bern-Rotterdam and j-Cypher registries. *EuroIntervention*. 2015;11:533-40.
23. Gutiérrez-Chico JL, Wykrzykowska J, Nüesch E, van Geuns RJ, Koch KT, Koolen JJ, di Mario C, Windecker S, van Es GA, Gobbens P, Juni P, Regar E, Serruys PW. Vascular tissue reaction to acute malapposition in human coronary arteries: sequential assessment with optical coherence tomography. *Circ Cardiovasc Interv*. 2012;5:20-9, s1-8.
24. Serruys PW, Onuma Y, Dudek D, Smits PC, Koolen J, Chevalier B, de Bruyne B, Thuesen L, McClean D, van Geuns RJ, Windecker S, Whitbourn R, Meredith I, Dorange C, Veldhof S, Hebert KM, Sudhir K, Garcia-Garcia HM, Ormiston JA. Evaluation of the second generation of a bioresorbable everolimus-eluting vascular scaffold for the treatment of de novo coronary artery stenosis: 12-month clinical and imaging outcomes. *J Am Coll Cardiol*. 2011;58:1578-88.
25. de Jaegere P, Mudra H, Figulla H, Almagor Y, Doucet S, Penn I, Colombo A, Hamm C, Bartorelli A, Rothman M, Nobuyoshi M, Yamaguchi T, Voudris V, DiMario C, Makovski S, Hausmann D, Rowe S, Rabinovich S, Sunamura M, van Es GA. Intravascular ultrasound-guided optimized stent deployment. Immediate and 6 months clinical and angiographic results from the Multicenter Ultrasound Stenting in Coronaries Study (MUSIC Study). *Eur Heart J*. 1998;19:1214-23.
26. Brugaletta S, Gogas BD, Garcia-Garcia HM, Farooq V, Girasis C, Heo JH, van Geuns RJ, de Bruyne B, Dudek D, Koolen J, Smits P, Veldhof S, Rapoza R, Onuma Y, Ormiston J, Serruys PW. Vascular compliance changes of the coronary vessel wall after bioresorbable vascular scaffold implantation in the treated and adjacent segments. *Circ J*. 2012;76:1616-23.

27. Gomez-Lara J, Brugaletta S, Farooq V, Onuma Y, Diletti R, Windecker S, Thuesen L, McClean D, Koolen J, Whitbourn R, Dudek D, Smits PC, Chevalier B, Regar E, Veldhof S, Rapoza R, Ormiston JA, Garcia-Garcia HM, Serruys PW. Head-to-head comparison of the neointimal response between metallic and bioresorbable everolimus-eluting scaffolds using optical coherence tomography. *JACC Cardiovasc Interv.* 2011;4:1271-80.

28. Sabate M, Windecker S, Iniguez A, Okkels-Jensen L, Cequier A, Brugaletta S, Hofma SH, Raber L, Christiansen EH, Suttrop M, Pilgrim T, Anne van Es G, Sotomi Y, Garcia-Garcia HM, Onuma Y, Serruys PW. Everolimus-eluting bioresorbable stent vs. durable polymer everolimus-eluting metallic stent in patients with ST-segment elevation myocardial infarction: results of the randomized ABSORB ST-segment elevation myocardial infarction-TROFI II trial. *Eur Heart J.* 2016;37:229-40.

29. Sotomi Y, Tateishi H, Suwannasom P, Dijkstra J, Eggermont J, Liu S, Tenekecioglu E, Zheng Y, Abdelghani M, Cavalcante R, de Winter RJ, Wykrzykowska JJ, Onuma Y, Serruys PW, Kimura T. Quantitative assessment of the stent/scaffold strut embedment analysis by optical coherence tomography. *Int J Cardiovasc Imaging.* 2016;32:871-83.

Supplementary data

Online Appendix 1. OCT analysis methods.

Online Table 1. Baseline characteristics.

Online Table 2. Summary of VLST cases.

Online Table 3. Quantitative coronary angiographic results of OCT-1 subgroup (full analysis set).

Online Appendix 2. Detailed description of VLST cases (non-OCT subgroup).

Online Figure 1. VLST case 1 (day 494).

Online Figure 2. VLST case 2 (day 536).

Online Figure 3. VLST case 3 (day 595).

Online Figure 4. VLST case 4 (day 679).

Online Appendix 3. Detailed description of subacute ST cases in the OCT-1 subgroup.

Online Figure 5. Subacute ST case 1.

Online Figure 6. Subacute ST case 2.

The supplementary data are published online at:

<http://www.pcronline.com/>

[eurointervention/106th_issue/180](http://www.pcronline.com/eurointervention/106th_issue/180)



Supplementary data

Online Appendix 1. OCT analysis methods

Quantitative assessment of the stented/scaffolded coronary segment of the final OCT pullback was performed in an independent core laboratory (Cardialysis BV, Rotterdam, The Netherlands) using QIvus software, version 3.0 (Medis, Leiden, The Netherlands). Taking into account the difference in optical properties of cobalt-chromium and polylactide, OCT analysis was performed using comparative methods¹¹. OCT imaging endpoints included the mean and minimal scaffold/stent and diameter, area and volume, the frequency of incomplete strut apposition including area and volume, the percentage of uncovered struts, the percentage of malapposed struts, the mean neointima thickness and neointimal hyperplasia area on top of the strut and inter-strut, and volume, the mean flow area and volume, the malapposition area and volume, and intraluminal defect area and volume⁵.

The malapposition distance was assessed as the distance between the interpolated lumen contour and the midpoint of the backside of the malapposed polymeric or metallic struts (abluminal reflective frame in polymeric struts or virtual backside of the metallic struts based on the strut thickness [XIENCE: 89 μm])¹¹. A malapposition distance greater than zero was the criterion of malapposition. Struts

were classified as uncovered if any part of the strut was visibly exposed to the lumen or as covered if a layer of tissue was visible over all the reflecting surfaces²³. Regarding polymeric struts, the threshold for coverage at follow-up was defined as 30 microns, which corresponds to the average interobserver measurement (difference in 300 struts analysed two times, $35\pm 6 \mu\text{m}$) of the endoluminal light backscattering frame of the strut²⁴. Eccentricity index (EI) was calculated per cross-section as the ratio of the projected minimal and maximal lumen or scaffold/stent diameter^{25,26}. Asymmetry index (AI) was calculated per lesion as $(1 - \text{projected minimum lumen or scaffold/stent diameter} / \text{projected maximal lumen or scaffold/stent diameter throughout an entire pullback})$ ²⁶.

Additionally, the following analyses were performed. Frequency of acute disruption and late discontinuities were assessed according to the previously published methods⁸. Qualitative assessment of the pattern of coverage was assessed at the site of the maximal in-stent/in-scaffold area obstruction in each lesion²⁷. To quantify the degree of vascular healing status, the healing score (%HS) was calculated using published methods^{10,28}. The degree of strut embedment was quantified using QCU-CMS (LKEB, Leiden, The Netherlands)²⁹.

Online Table 1. Baseline characteristics.

Patients		Entire study population		OCT-1 subgroup	
		BVS	CoCr-EES	BVS	CoCr-EES
		N=266	N=134	N=82	N=43
Age (years)		67.1±9.4	67.3±9.6	65.8±9.8	67.6±11.2
Male gender		210 (78.9%)	99 (73.9%)	65 (79.3%)	31 (72.1%)
Body mass index (kg/m ²)		24.0±3.0	24.3±3.0	24.3±3.2	24.0±2.7
Current smoker		53 (19.9%)	29 (21.6%)	17 (20.7%)	8 (18.6%)
Hypertension		208 (78.2%)	107 (79.9%)	65 (79.3%)	37 (86.0%)
Dyslipidaemia		218 (82.0%)	110 (82.1%)	68 (82.9%)	35 (81.4%)
Diabetes		96 (36.1%)	48 (35.8%)	31 (37.8%)	18 (41.9%)
Treated with insulin		24 (9.0%)	11 (8.2%)	6 (7.3%)	2 (4.7%)
HbA1c (%)		6.2±1.1	6.2±0.8	6.1±0.8	6.2±0.6
Prior intervention to target vessel		9 (3.4%)	7 (5.2%)	2 (2.4%)	1 (2.3%)
Previous myocardial infarction		42/262 (16.0%)	32 (23.9%)	13 (16.3%)	8 (18.6%)
Current evidence of ischaemia	Stable angina	170 (63.9%)	88 (65.7%)	57 (69.5%)	29 (67.4%)
	Unstable angina	26 (9.8%)	22 (16.4%)	5 (6.1%)	7 (16.3%)
	Silent ischaemia	70 (26.3%)	24 (17.9%)	20 (24.4%)	7 (16.3%)
Number of target lesions	One	257 (96.6%)	131 (97.8%)	78 (95.1%)	42 (97.7%)
	Two	9 (3.4%)	3 (2.2%)	4 (4.9%)	1 (2.3%)
	Non-study lesions treated	20 (7.5%)	10 (7.5%)	4 (4.9%)	4 (9.3%)
Target lesions		N=275	N=137	N=86	N=44
Left anterior descending		127 (46.2%)	58 (42.3%)	45 (52.3%)	20 (45.5%)
Left circumflex/ramus		63 (22.9%)	36 (26.3%)	16 (18.6%)	14 (31.8%)
Right coronary artery		85 (30.9%)	43 (31.4%)	25 (29.1%)	10 (22.7%)
Calcification (moderate/severe)		76/274 (27.7%)	45 (32.8%)	19 (22.4%)	15 (34.1%)
Calcification (severe)		19/274 (6.9%)	15 (10.9%)	8 (9.3%)	6 (13.6%)
Tortuosity (moderate/severe)		23/274 (8.5%)	11 (8.0%)	6 (7.1%)	4 (9.1%)
Eccentric lesion		223/273 (81.7%)	113 (82.5%)	77 (90.6%)	35 (79.5%)
ACC/AHA lesion classification	A	11 (4.0%)	5 (3.6%)	3 (3.5%)	1 (2.3%)
	B1	55 (20.0%)	28 (20.4%)	14 (16.3%)	7 (15.9%)
	B2	154 (56.0%)	68 (49.6%)	51 (59.3%)	23 (52.3%)
	C	55 (20.0%)	36 (26.3%)	18 (20.9%)	13 (29.5%)

ACC/AHA: American College of Cardiology/American Heart Association; BVS: bioresorbable vascular scaffold; CoCr-EES: cobalt-chromium everolimus-eluting stents; OCT: optical coherence tomography

Online Table 2. Summary of VLST cases.

Case	1	2	3	4
Clinical characteristics				
Age	79 years	44 years	72 years	59 years
Gender	Male	Male	Male	Male
Diabetes	YES	YES	YES	YES
ACS at the index procedure	NO: CCS class I	NO: CCS class I	NO: CCS class III	NO: CCS class II
Type of P2Y ₁₂ inhibitor prescribed	Clopidogrel	Clopidogrel	Clopidogrel	Clopidogrel
Angiographic and procedural characteristics				
Treated lesion location	Proximal LAD	Mid RCA	Distal RCA	Distal RCA
AHA/ACC lesion type	B2	C	B2	B1
Bifurcation	YES: 1,0,0	YES: 0,1,1	NO	NO
Pre-procedural QCA				
Minimum lumen diameter	1.64 mm	0.51 mm	0.54 mm	1.14 mm
Reference vessel diameter	3.16 mm	3.37 mm	2.94 mm	3.14 mm
Lesion angulation	0°	37°	20°	15°
Procedural details				
Post-procedural OCT	NO	NO	NO	NO
Post-procedural IVUS	NO	YES	NO	NO
Predilatation	YES	YES	YES	YES
Size of predilatation balloon	3.0×15 mm	3.5×12 mm	2.75×10 mm	3.0×12 mm
Maximum inflation pressure	12 atm	14 atm	20 atm	10 atm
Non-compliant balloon use	NO	NO	YES	NO
Expected balloon diameter	3.07 mm	3.7 mm	2.89 mm	3.01 mm
Device implantation	Size of implanted BVS			
	3.5×28 mm	3.5×18 mm	3.0×18 mm	3.5×18 mm
	Number of BVS implanted			
	1	1	1	1
	Implantation pressure			
	10 atm	15 atm	8 atm	14 atm
	Expected balloon diameter			
	3.78 mm	3.98 mm	3.08 mm	3.94 mm
Post-dilatation	YES	NO	YES	NO
	Size of post-dilatation balloon		3.25×10 mm	
	Maximum inflation pressure		16 atm	
	Non-compliant balloon use		YES	
	Expected balloon diameter		3.37 mm	
Post-procedural QCA				
In-segment percent diameter stenosis	18.1%	16.2%	20.5%	7.6%
In-segment minimum lumen diameter	2.57 mm	2.79 mm	2.19 mm	3.12 mm
In-device percent diameter stenosis	18.1%	16.2%	11.1%	4.5%
In-device minimum lumen diameter	2.57 mm	2.79 mm	2.45 mm	3.23 mm
1-year QCA				
In-segment percent diameter stenosis	22.6%	11.0%	22.4%	20.1%
In-segment minimum lumen diameter	2.24 mm	2.79 mm	2.61 mm	2.18 mm
In-device percent diameter stenosis	13.0%	2.2%	22.4%	8.4%
In-device minimum lumen diameter	2.52 mm	3.06 mm	2.61 mm	2.50 mm
Information at time of VLST				
Time interval from the index procedure to VLST	494 days	536 days	595 days	679 days
Antithrombotic medications	Aspirin	NO (for 7 days)	YES	YES
	P2Y ₁₂ inhibitor	NO	NO	YES
	Oral anticoagulant	NO	NO	NO
OCT findings				
OCT at or after the event	YES	NO (IVUS)	YES (5 days after VLST)	
Incomplete lesion coverage	NO	–	NO	NO
Malapposition	YES	–	YES	YES
Restenosis due to neointimal growth	NO	–	NO	NO
Strut discontinuity (stacked or overhanging struts)	YES	–	YES	YES
Underexpansion (minimum scaffold area/reference area <0.7)	NO	–	NO	NO
ACS: acute coronary syndrome; AHA/ACC: American Heart Association/American College of Cardiology; BVS: bioresorbable vascular scaffold; CCS: Canadian Cardiovascular Society; IVUS: intravascular ultrasound; LAD: left anterior descending coronary artery; OCT: optical coherence tomography; QCA: quantitative coronary angiography; RCA: right coronary artery; VLST: very late stent/scaffold thrombosis				

Online Table 3. Quantitative coronary angiographic results of OCT-1 subgroup (full analysis set).

	BVS	CoCr-EES	p-value
Baseline			
Number of lesions	85	44	
Lesion length (mm)	13.9±5.5	13.4±5.0	0.65
Reference vessel diameter (mm)	2.69±0.44	2.76±0.50	0.43
MLD (mm)	0.95±0.36	0.98±0.34	0.58
DS (%)	64.6±12.5	64.4±9.9	0.91
Post-procedure			
Number of lesions	86	44	
Reference vessel diameter (mm)	2.74±0.42	2.83±0.45	0.27
In-segment MLD (mm)	2.20±0.40	2.23±0.51	0.78
In-device MLD (mm)	2.42±0.39	2.58±0.43	0.031
In-segment DS (%)	19.6±7.0	21.6±10.2	0.24
In-device DS (%)	11.7±7.1	8.5±7.0	0.015
In-segment acute gain (mm)	1.26±0.42*	1.25±0.50	0.9
In-device acute gain (mm)	1.47±0.44*	1.60±0.42	0.085
Follow-up at 13 months			
Number of lesions	83	41	
Reference vessel diameter (mm)	2.68±0.41	2.79±0.50	0.21
In-segment MLD (mm)	2.04±0.43	2.16±0.61	0.27
In-device MLD (mm)	2.20±0.44	2.46±0.60	0.017
In-segment DS (%)	23.8±10.2	23.3±13.6	0.84
In-device DS (%)	17.8±9.9	12.2±13.3	0.021
In-segment binary restenosis	1 (1.2%)	2 (4.9%)	0.25
In-device binary restenosis	1 (1.2%)	1 (2.4%)	1
In-segment late lumen loss (mm)	0.17±0.29	0.06±0.33	0.072
In-device late lumen loss (mm)	0.22±0.26	0.12±0.35	0.09
Follow-up at 24 months			
Number of lesions	77	40	
Reference vessel diameter (mm)	2.68±0.43	2.77±0.50	0.35
In-segment MLD (mm)	1.95±0.49	2.10±0.51	0.14
In-device MLD (mm)	2.08±0.56	2.37±0.58	0.01
In-segment DS (%)	27.7±12.2	24.7±10.2	0.16
In-device DS (%)	23.3±13.0	14.8±11.9	0.0006
In-segment binary restenosis	6 (7.8%)	1 (2.5%)	0.42
In-device binary restenosis	4 (5.2%)	1 (2.5%)	0.66
In-segment late lumen loss (mm)	0.27±0.38	0.12±0.32	0.029
In-device late lumen loss (mm)	0.36±0.38	0.21±0.38	0.04

* N=85. Data are expressed as mean±standard deviation, or number (percentage). BVS: bioresorbable vascular scaffold; CoCr-EES: cobalt-chromium everolimus-eluting stent; DS: diameter stenosis; MLD: minimal lumen diameter

Online Appendix 2. Detailed description of VLST cases (non-OCT subgroup)

VLST CASE 1 (DAY 494)

The subject is a 79-year-old male, former smoker with a history of dyslipidaemia and hypertension, both requiring medication, type 2 diabetes mellitus treated with oral hypoglycaemics, Canadian Cardiovascular Society (CCS) class I stable angina. The core lab assessed a moderately calcified 17.86 mm lesion in the proximal left anterior descending artery (LAD) involving a side branch, with reference vessel diameter (RVD) of 3.65 mm proximal and 2.76 mm distal (**Online Figure 1A**). On 18 December 2013, the subject was enrolled in the trial and received one 3.5×28 mm bioresorbable vascular scaffold (BVS) at 10 atm in the proximal LAD followed by post-dilatation using a 3.5×15 mm non-compliant balloon at 18 atm. Final in-scaffold minimal lumen diameter (MLD) was 2.57 mm with 18% diameter stenosis (%DS) without angiographic complications (**Online Figure 1B**). Protocol-required 13-month coronary angiography showed no restenosis at the target lesion (13.0% in-scaffold %DS, and 22.6% in-segment %DS).

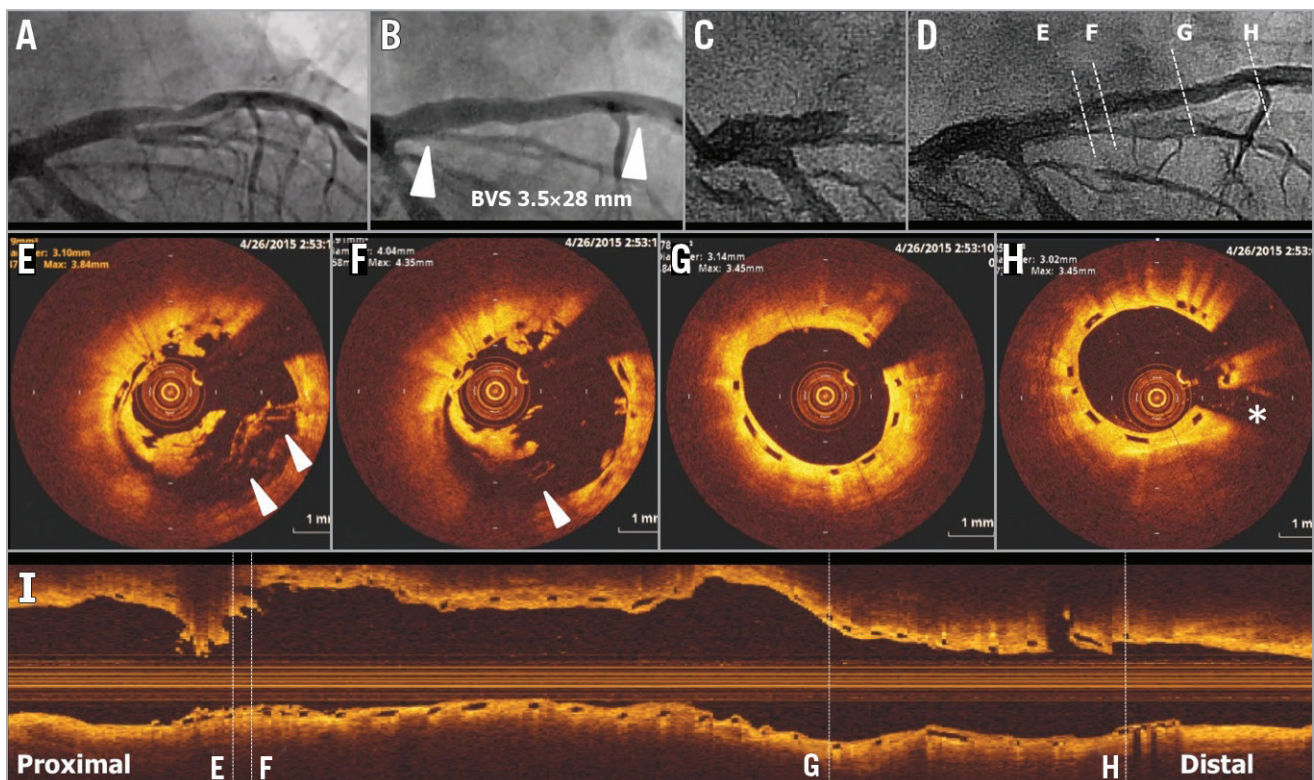
On day 494, the subject returned to the hospital due to acute Q-wave myocardial infarction. Coronary angiography showed acute occlusion of the LAD at the proximal edge of the scaffold (**Online Figure 1C**). After successful manual thrombus aspiration (**Online Figure 1D**), OCT showed overhanging struts and uncovered malapposed struts with a disruption of circularity at the proximal part of the scaffold (**Online Figure 1E, Online Figure 1F**). The middle and distal parts of the scaffold showed no remarkable findings (**Online**

Figure 1G, Online Figure 1H, Online Figure 1I). A metallic stent was implanted without complications. Clopidogrel and cilostazol had already been discontinued after one-year follow-up, whereas aspirin was discontinued one week prior to the event but no reason was indicated.

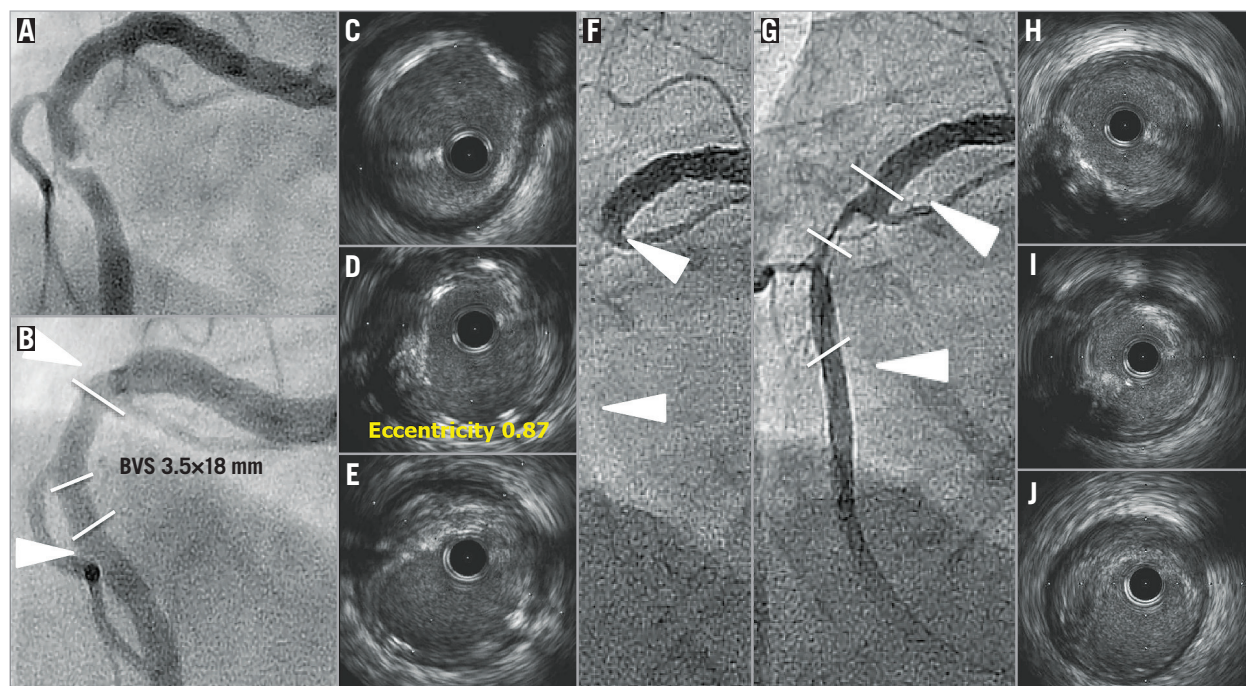
VLST CASE 2 (DAY 536)

The subject is a 44-year-old male, with a history of hypertension and dyslipidaemia, both requiring medication, type 2 diabetes mellitus treated with oral hypoglycaemics, CCS class I stable angina. Core lab assessed a moderately calcified 6.93 mm lesion in the mid right coronary artery (RCA) involving a small ventricular branch, with RVD of 3.15 mm proximal and 3.58 mm distal (**Online Figure 2A**). On 27 June 2013, the subject received a 3.5×18 mm BVS at 15 atm in the mid RCA without post-dilatation. Final in-segment MLD was 2.79 mm with a %DS of 16.2% without angiographic complications (**Online Figure 2B**). The patient was sub-randomised to the intravascular ultrasound (IVUS) subgroup and therefore post-procedural IVUS was performed. On IVUS, no apparent malapposition was observed and minimal lumen area was 7.95 mm² (**Online Figure 2C-Online Figure 2E**). Protocol-required 13-month coronary angiography showed no restenosis (22% in-scaffold %DS).

On day 536, the subject presented with an ST-segment elevation myocardial infarction (STEMI) without abnormal Q-waves. Coronary angiography revealed occlusion of the RCA at the proximal edge of the scaffold (**Online Figure 2F**). After successful manual thrombus aspiration (**Online Figure 2G**), IVUS revealed



Online Figure 1. VLST case 1 (day 494).



Online Figure 2. VLST case 2 (day 536).

protruding tissues with attenuation in the scaffolded segment without apparent strut malapposition (**Online Figure 2H-Online Figure 2J**). A bare metal stent was implanted. Clopidogrel had been discontinued at one year, whereas aspirin was ongoing after interruption in days 433-461 due to planned surgery.

VLST CASE 3 (DAY 595)

The subject is a 72-year-old male, former smoker with a history of type 2 diabetes mellitus treated with oral hypoglycaemics, CCS class III stable angina. Core lab assessed a mildly calcified 6.91 mm lesion in the distal RCA with an RVD of 3.07 mm proximal and 2.81 mm distal (**Online Figure 3A**). The patient received a 3.0×18 mm BVS at 8 atm in the distal RCA followed by post-dilatation with a 3.25×10 mm non-compliant balloon at 16 atm. Final in-segment MLD was 2.19 mm with a %DS of 20.5% (**Online Figure 3B**). Protocol-required 13-month coronary angiography demonstrated in-scaffold %DS of 8.4%.

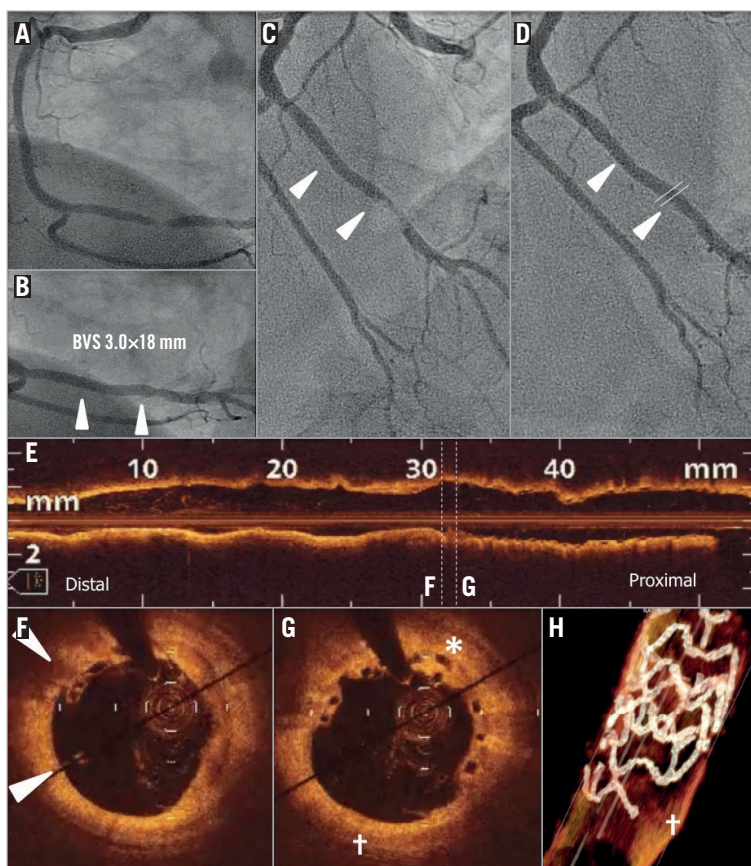
On day 595, the patient presented with an acute myocardial infarction (**Online Figure 3C**). Coronary angiography revealed an occlusive thrombus at the distal edge of the scaffold. Manual thrombus aspiration was performed, which improved the Thrombolysis In Myocardial Infarction (TIMI) flow up to 2 with a distal embolisation of the atrioventricular branch. Five days after VLST, the patient came back to the catheterisation laboratory (**Online Figure 3D**), which revealed restoration of flow (TIMI 3). OCT demonstrated malapposed struts in the distal part of the scaffold (arrowhead, **Online Figure 3F**) and covered overhanging struts (asterisk, **Online Figure 3G**). One half of the distal ring was not discernible (+ in **Online Figure 3H**) by three-dimensional OCT reconstruction, and it is speculated that the ring was dislocated by wire and thrombus

aspiration. Distal to the scaffold, OCT revealed a calcified and light-attenuating plaque without significant stenosis.

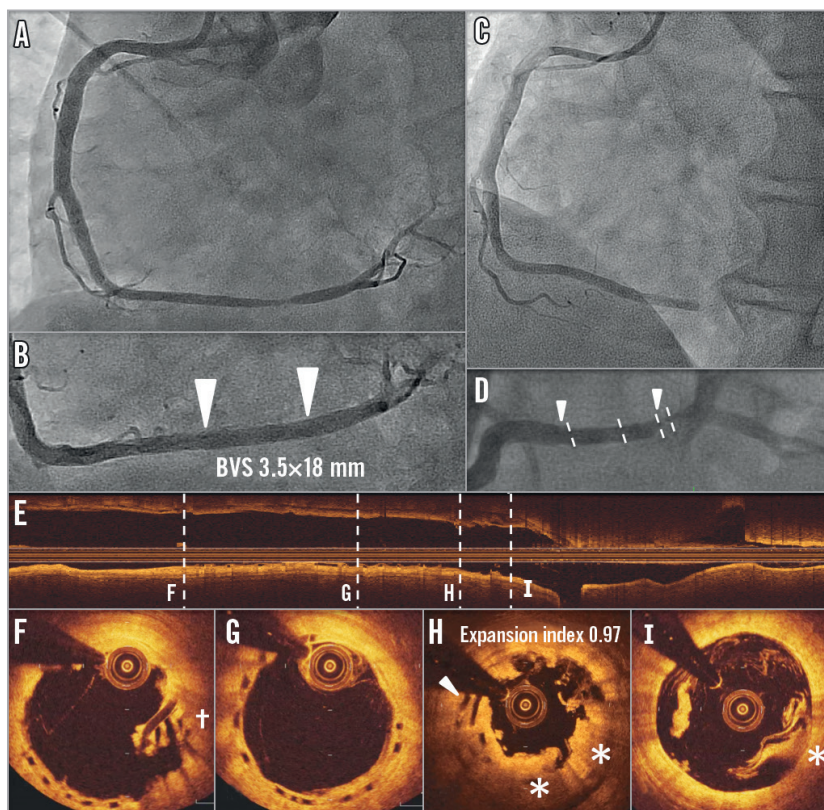
VLST CASE 4 (DAY 679)

The subject is a 59-year-old male, smoker with a history of dyslipidaemia requiring medication, type 2 diabetes mellitus treated with oral hypoglycaemics, CCS class II stable angina. Core lab assessed a moderately calcified 10.84 mm lesion in the distal RCA (**Online Figure 4A**), with RVD of 3.08 mm proximal and 3.20 mm distal. The subject received a 3.5×18 mm BVS at 14 atm in the distal RCA without post-dilatation (**Online Figure 4B**). Final in-segment MLD was 3.12 mm with in-scaffold %DS of 7.6% and no dissection was observed. Protocol-required 13-month coronary angiography demonstrated no significant stenosis at the target lesion (2.2% in-scaffold %DS and 11% in-segment %DS).

On day 679, the subject returned to the hospital due to STEMI. Coronary angiography showed occlusion of the RCA at the distal edge of the scaffold (**Online Figure 4C**, **Online Figure 4D**). OCT after manual thrombus aspiration (**Online Figure 4E-Online Figure 4I**) revealed overhanging struts (**Online Figure 4I** and arrowhead in **Online Figure 4H**) with coverage by the light-attenuating tissue (* in **Online Figure 4H** and **Online Figure 4I**) or overhanging struts without coverage (+ in **Online Figure 4F**), demonstrating the presence of strut discontinuities. The procedure was completed after ballooning without implanting a metallic scaffold. Clopidogrel was discontinued at day 669 and aspirin was continued. The patient came back to the catheterisation laboratory 24 days later due to recurrent angina. OCT revealed overhanging struts without coverage remaining in the distal part of the scaffold. A metallic drug-eluting stent was implanted.



Online Figure 3. VLST case 3 (day 595).



Online Figure 4. VLST case 4 (day 679).

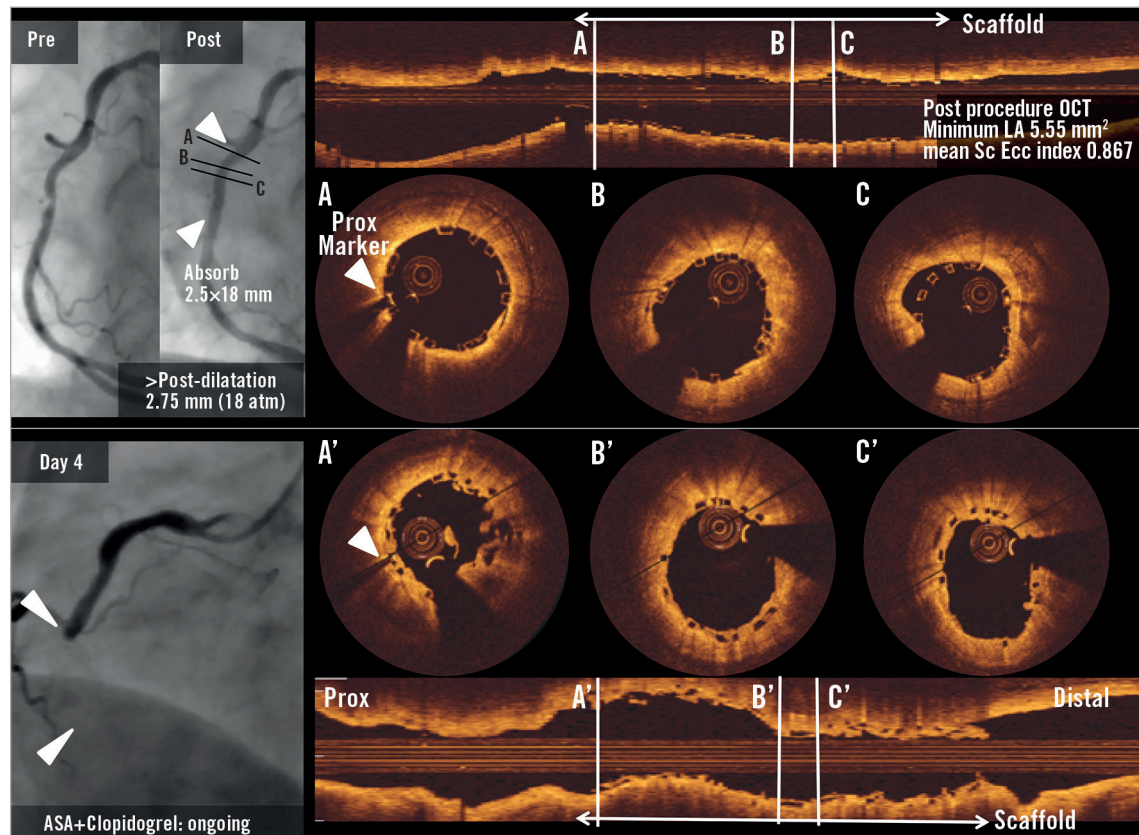
Online Appendix 3. Detailed description of subacute ST cases in the OCT-1 subgroup

SUBACUTE ST CASE 1

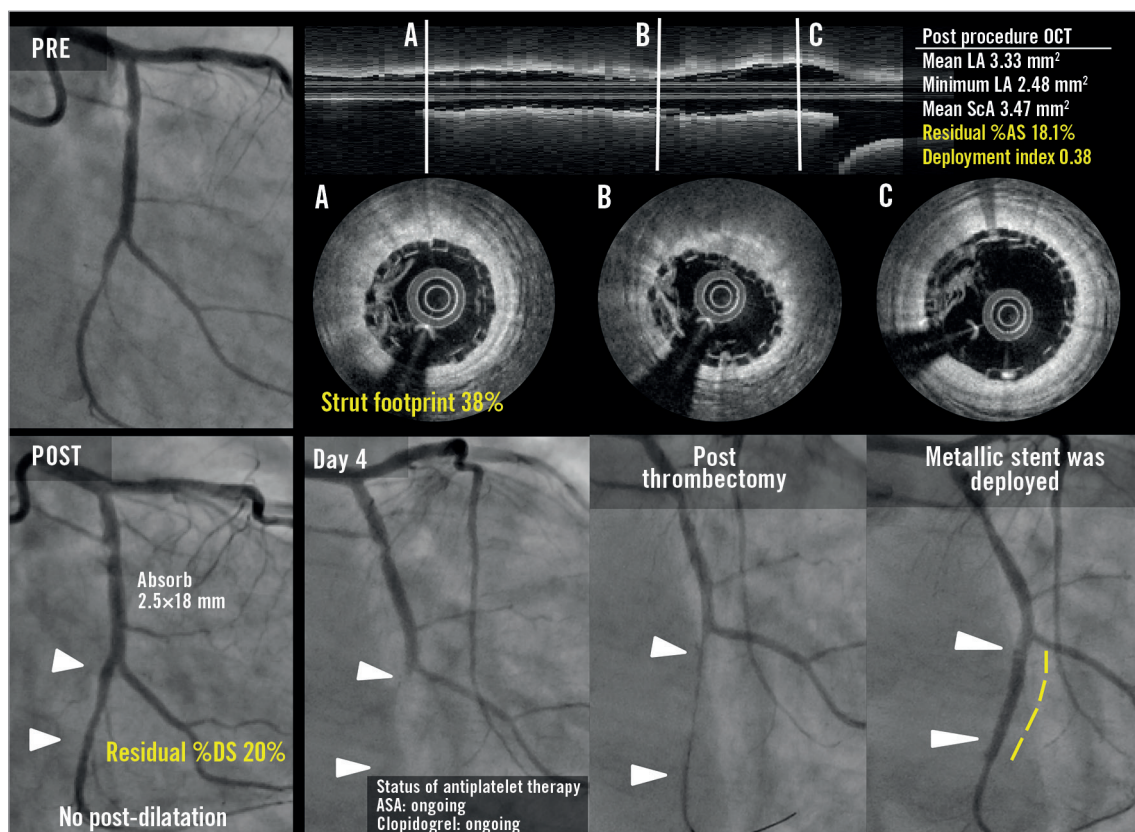
A 64-year-old male smoker with a history of dyslipidaemia and hypertension, type 2 diabetes mellitus treated with oral hypoglycaemics, and CCS class II stable angina was treated with a 2.5×18 mm BVS implantation in the mid RCA with post-dilatation by a 2.75 mm balloon. Post-procedural OCT (**Online Figure 5A-Online Figure 5C**) showed a good expansion of the scaffold (minimal LA: 5.55 mm²) with a small malapposition in the middle part of the scaffold. On day four, the patient presented with non-Q-wave myocardial infarction, with angiographic occlusion in the proximal edge of the scaffold. Post-thrombectomy OCT (**Online Figure 5A'-Online Figure 5C'**) showed an attachment of tissue in the proximal part with resolution of malapposition in the middle part. Aspirin and clopidogrel were ongoing.

SUBACUTE ST CASE 2

A 64-year-old male with a history of dyslipidaemia requiring medication, hypertension, previous drug-eluting stent implantation in a non-target vessel, former tobacco use presented with a CCS class II stable angina. The patient received a 2.5×18 mm BVS scaffold in a relatively small left circumflex coronary artery without post-dilatation. Post-procedural OCT showed an underexpansion of the 2.5 mm device with a minimum lumen area of 2.48 mm² and mean scaffold area of 3.47 mm² with a high density of polymeric struts (**Online Figure 6A-Online Figure 6C**). Post-procedural angiographic residual stenosis was 20%. The patient developed STEMI on day four, and coronary angiography showed in-scaffold occlusion at the proximal edge of the scaffold. The subacute scaffold thrombosis was treated by implantation of a metallic stent. Aspirin and clopidogrel were ongoing.



Online Figure 5. Subacute ST case 1.



Online Figure 6. Subacute ST case 2.